Colour detection thresholds as a function of chromatic adaptation and light level

B. J. Jennings
J. L. Barbur

Colour threshold discrimination ellipses were measured for a number of states of chromatic adaptation and a range of luminance levels using the Colour Assessment and Diagnosis (CAD) test. An analysis of these results was carried out by examining the cone excitation signals along the cardinal axes that correspond to detection thresholds in the +L-M (reddish), −L+M (greenish), +S (bluish) and −S (yellowish) colour directions. The results reveal a strong linear relationship between the excitations induced by the adapting background field in each cone class and the corresponding changes needed for threshold detection. These findings suggest that the cone excitation change for threshold detection of colour signals is always the same for a given background excitation level (in any cone class), independent of the excitations generated in the other cone classes. These observations have been used to develop a model to predict colour detection thresholds for any specified background luminance and chromaticity within the range of values investigated in this study (e.g., luminances in the range 0.3 to 31 $cd.m^{-2}$ and chromaticities within the gamut of typical CRT displays). Predicted colour thresholds were found to be in close agreement with measured values with errors that do not, in general, exceed the measured within-subject variability.

Introduction

When the light reflected from an object differs in spectral composition to the surrounding background field, these spectral differences are reflected in the excitation levels produced in each class of photoreceptor. The colour discrimination performance of the human eye is strongly affected by both the luminance level and the spectral composition of the adapting light (Yeh et al., 1993; Yebra et al., 2001). Knowledge of the limits of colour discrimination is important in setting safety standards and guidelines in visually-demanding workplace environments; for example, in aviation, rail and maritime transport. Varying conditions of illumination and chromatic adaptation are employed in different working environments and these will affect chromatic detection (Loomis and Berger, 1979; Hita et al., 1989). It is therefore of both fundamental and practical interest to be able to predict accurately how the subject's colour detection performance changes with light level and chromatic adaptation. The Colour Assessment and Diagnosis (CAD) test (Rodriguez-Carmona et al., 2005; Barbur et al., 2006) was used to measure colour detection threshold ellipses under different states of chromatic adaptation and background light levels. The advantage of this technique is that it isolates the use of colour signals in both normal trichromats and colour deficient observers by embedding the 'isoluminant' chromatic stimulus in dynamic luminance noise (Barbur, 2003). These threshold variations are analysed in terms of changes in L-, M- and S-cone excitation levels required for threshold in the +L-M, -L+M, +S and –S directions. A model based on the measured threshold chromatic sensitivity data is proposed to extend these data to other states of chromatic adaptation and retinal luminance levels within the limits investigated. The model is based on the measured relationships between colour detection thresholds and the corresponding cone excitations generated when varying the spectral composition and intensity of the background field.

Method

Equipment

The stimulus was displayed on a Multiscan 500PS Trinitron monitor (Sony Corporation, Tokyo, Japan); screen size 27° × 22°, using a frame rate of 75 Hz. The monitor was driven by an ELSA GLoria XL 30-bit graphics card (ELSA Optical Technology Inc. Aachen, Germany). The controlling software ran on a desktop PC running MS-DOS: the choice of operating system was to eliminate the risk of context switching, and hence ensure accurate timing for stimulus generation and display. Observers responded to the stimuli by pressing one of four buttons on a handheld control pad, this was connected to the PC via an PC30AT multifunction data acquisition card (Amplicon, Brighton, East Sussex, UK). A chin and forehead rest was used for convenience and to maintain a fixed eye to monitor distance of 700 mm.

The CAD test uses spatiotemporal luminance noise to isolate the detection of colour signals (Barbur, 2003). The stimulus is composed of a 5 × 5 square array of checks, of which 21 are coloured and move diagonally in a randomly selected direction. The stimulus moves at a constant speed of ~4°/s, over a visual angle of ~2.9°, across a larger square region of 3.3° defined by dynamic luminance contrast noise. The stimulus colour as specified by its CIE (x, y) co-ordinates had the same mean luminance as the background field and the Euclidian distance between background and test stimulus chromaticities provided a measure of colour signal strength. Sixteen different directions in CIE space were employed: 0, 22.5,…, 337.5°. The threshold was measured along each direction using one of 16 interleaved staircases. For each presentation the stimulus motion direction was chosen randomly. A larger background field of angular subtense 27° × 22°, and luminance equal to that of the stimulus provided the adapting field. A number of discrete background chromaticities and luminance levels were investigated.

The observer's task was to press one of four buttons arranged as a square (in a four-alternative, forced-choice procedure) to indicate the direction of movement (i.e., the button that corresponded to the corner of the square that the stimulus traveled towards). When unable to see the coloured stimulus, the observer was instructed to press any of the four buttons.

Selection of background chromaticities and luminance levels

Two main factors determined the choice of chromaticities for the twelve backgrounds employed in this study. The first was the chromaticities and the output luminance range of each of the monitor phosphors. At higher luminance levels the gamut of chromaticities available is reduced (Morovic, 2008), this limited the choice of background chromaticities for which colour detection thresholds could be measured. The second factor is the massive increase in colour detection thresholds at lower luminance levels (Walkey et al., 2001). This increase can cause the thresholds to fall outside the gamut of the display. The twelve background chromaticities were chosen to cover as much of the display gamut as possible, within its chromaticity and luminance limits, whilst also ensuring that the measured colour detection thresholds also fall within these limits. Colour threshold ellipses could be measured for nearly every selected background in the range 1–31 $cd.m^{-2}$. At the lowest light level investigated, i.e., 0.3 $cd.m^{-2}$, only four of the 12 backgrounds could be measured. A

spectrally calibrated neutral density filter of optical density 1 unit was employed when testing at luminance levels of 3 cd.m^{-2} and below.

Experimental procedure and data processing

Four subjects took part in this study; all had normal colour vision according to the CAD test and also produced Nagel anomaloscope matches in the normal range. All subjects had 6/6 vision or better and wore appropriate refractive correction, if required. Each observer carried out the CAD test for each background chromaticity and luminance level employed in the study. Adaptation to the uniform background field for 90 s preceded the tests, except those for the lowest background luminance levels when the subject adapted for 20 min. The testing was carried out over a number of sessions. The results for the four subjects were averaged for each background and luminance level and for each of the 16 colour directions tested. The measured ellipses become asymmetric at the very low light levels, mainly due to an increased threshold in the yellow direction, as also shown previously by Brown (1951). These observations have been taken to reflect differences in sensitivity for increments and decrements in S-cone signals at low light levels (Walkey et al., 2001; Yebra et al., 2001). The ellipse-fitting algorithm employed in this study predicts well the measured thresholds, but a (least-squares) fitting algorithm with a non-fixed center needs to be employed (Fitzgibbon et al., 1999) in order to preserve asymmetric elongations. This procedure yielded a result set containing the semi-major, a, and semi-minor, b, ellipse axes; the orientation of the major axis relative to the abscissa; and the fitted ellipse centre co-ordinates (x_o, y_o). The coordinates in CIE space of R_t, G_t, B_t and Y_t (shown in Figure 1) were determined using standard parametric ellipse equations (Salomon, 2005). These values are shown later to represent the thresholds in the +L-M, -L+M, +S and –S directions, respectively, once transformed into cone excitation space. Figure 1 also shows the positions of these points relative to the background chromaticity (x_{bg}, y_{bg}) and fitted ellipse centre (x_o, y_o).
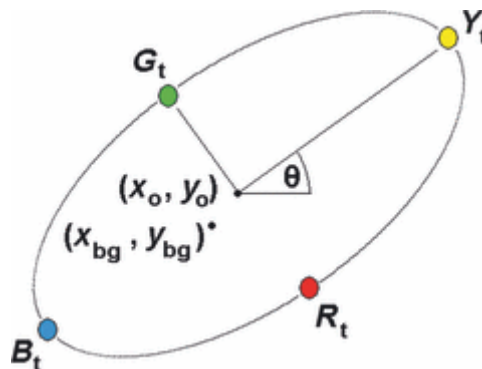

Figure 1
The four threshold coordinates R_t, G_t, Y_t and B_t calculated from the fitted ellipse in CIE space, with respect to the ellipse orientation and fitted centre (x_o, y_o). The specified background coordinate is at (x_{bg}, y_{bg}).

These four CIE threshold coordinates along with the CIE background coordinates (not fitted ellipse center co-ordinates) were transformed into their corresponding CIE XYZ tristimulus

values (Hunt, 1998). These in turn, were then transformed into L-, M- and S-cone excitations using Equation 1.

$$\begin{bmatrix} L \\ M \\ S \end{bmatrix} = Q \begin{bmatrix} X \\ Y \\ Z \end{bmatrix}$$

(Equation 1)

The multiplier Q is a 3×3 matrix that is calculated using the method outlined by Golz and MacLeod (2003). We use the Stockman and Sharpe (2000) cone fundamentals and the measured relative radiance distributions of the red, green and blue phosphor guns of the Sony monitor as inputs. This method was verified by calculating cone excitations from first principles. The computation was performed by individually integrating over the visible spectrum the product of the L-, M- and S-cone fundamentals and the corresponding spectral radiance distributions needed to generate the specified background and target chromaticities. This procedure yielded the excitation in each cone class produced by targets and backgrounds which were found to be within 0.5% of the corresponding values computed using the Golz and MacLeod (2003) matrix method.

Results

All mean CAD measured ellipses in CIE space were transformed into the [L-M]- vs S-excitation space and are shown in Figure 2. This plot shows the [L-M]- vs S-cone excitations in the horizontal plane as a function of background luminance (cd m^{-2}) in the vertical plane. A linear model of cone excitation is assumed and hence the L:M:S cone excitation ratio remains constant as the background luminance level varies. This means that the ratio of [L-M] to S will also stay constant. For a given background chromaticity the co-ordinates of the background excitations in the [L-M]- vs S-cone excitation plane fall onto a straight line as a function of background luminance. This curve will always point in the direction of the origin (0, 0, 0). Hence a diagonal straight line can be plotted through the 3D excitation space that represents a constant chromaticity, but varying luminance. This is illustrated by the black solid line in Figure 2, connecting the CIE (x, y): 0.305, 0.323 background chromaticity at different luminance levels.
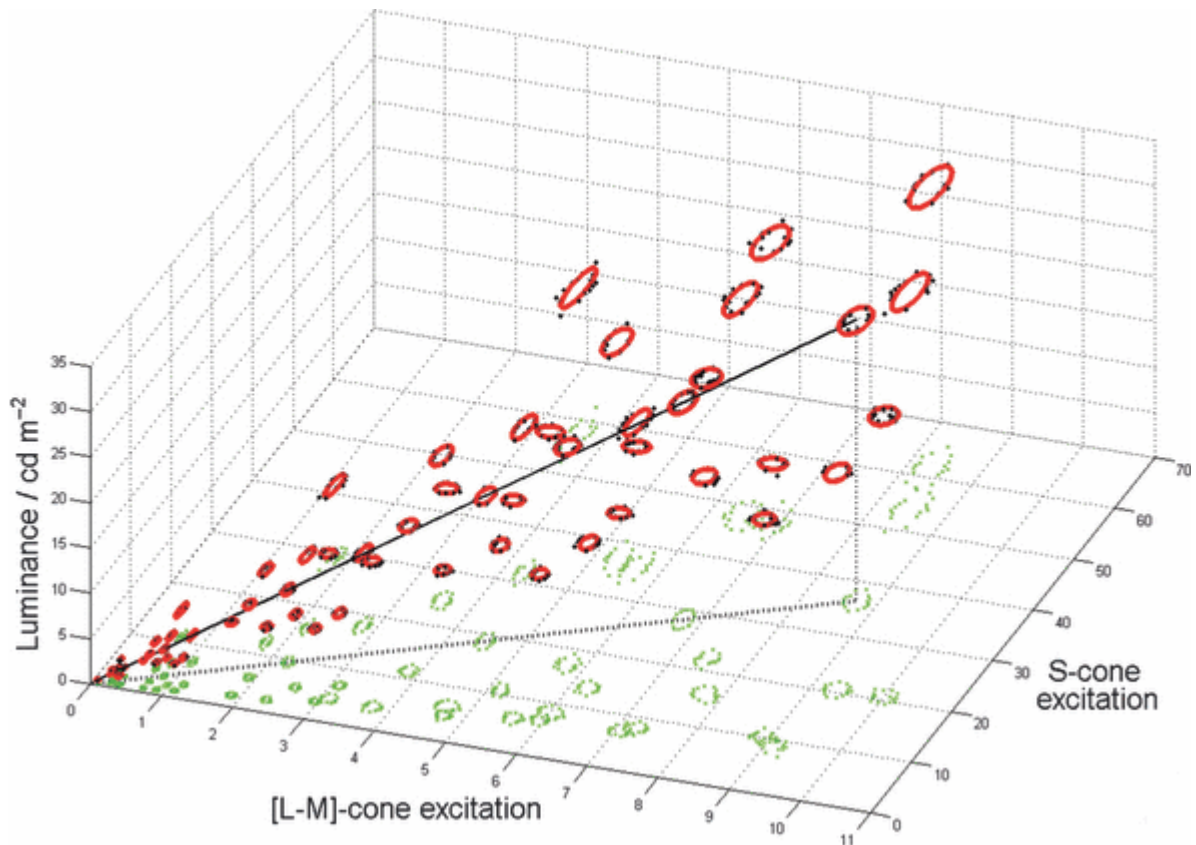
Figure 2
*Measured ellipse data (averaged over four subjects) and represented as [L-M]- vs S-cone
excitations are plotted as a function of background luminance. The black dots represent the
mean measured data; the green crosses represent the projection of these measured points
onto the zero luminance plane for clarity. The fitted ellipses for each background are shown
in red and the black solid line shows how points of constant chromaticity plot over the
luminance range investigated in this study. For the case illustrated, the black line
corresponds to CIE (x, y)- coordinates 0.305, 0.323.*

Variation in detection thresholds

L- and M-cones. The L-, M- and S-cone excitations were calculated for each background
(L_b, M_b and S_b, respectively), at each of the luminance levels, along with the corresponding
L-, M- and S-cone threshold excitations (L_t, M_t and S_t, respectively) in the $+[L-M]$, $-[L-M]$,
$+S$ and $-S$ cardinal directions. The corresponding changes in L- and M-cone excitations
required for threshold in the $+L - M$ direction are illustrated in Figure 3. The x-axis
represents the excitations produced in the L- and M-cones (L_b and M_b) by the different
background chromaticities and luminance levels employed. The y-axis plots the increments in
L- and M-cones needed to reach threshold (δL and δM, respectively, where $\delta L = L_t - L_b$
and $\delta M = M_t - M_b$). The slight clustering of the data points along the curves corresponds
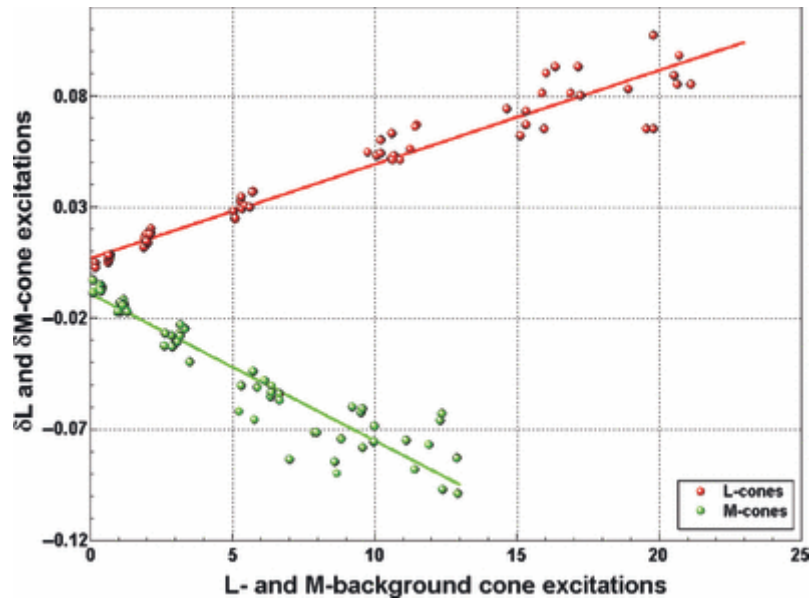to the different background luminance levels employed.

Figure 3

The changes required in L- and M-cone excitations for threshold in the +L-M cardinal direction vs the L- and M-excitations produced by the backgrounds. The data shown represent the range of luminance levels and background chromaticities investigated in the study.

The data show a strong linear relationship between the L- and M-cone excitations produced by the background and the corresponding excitation changes required for threshold for all chromatic backgrounds and luminance levels in the measured range (r^2 = 0.94 and 0.90 for the L-cone and M-cones, respectively).

Equations 2 and 3 are based on Figure 3 and are used by the model to predict the amounts by which the stimulus L-cone excitation must increase (Equation 2) and the corresponding M-cone excitation must decrease (Equation 3) to reach threshold in the +L-M direction, based only on the background excitations.

$$\delta L = 0.0042L_b + 0.0071 \qquad \text{(Equation 2)}$$
$$\delta M = -0.0066M_b - 0.0086 \qquad \text{(Equation 3)}$$

Similar sets of curves were produced for the –L+M direction using the same method. From these plots, Equations 4 and 5 were determined. These equations predict the positive/negative L- and M-cone increments needed to reach threshold when S-cone changes are absent or negligible.

$$\delta L = -0.0044L_b + 0.0084 \qquad \text{(Equation 4)}$$
$$\delta M = 0.0069M_b + 0.0081 \qquad \text{(Equation 5)}$$

Equations 2, 3, 4 and 5 illustrate that the L- and M-cone excitation changes required for threshold are equal and opposite in the +L-M and –L+M directions.

S-Cones

The change in the excitation of S-cones needed to reach threshold in the +S direction follows a similar linear relationship (r^2 = 0.96) as the L- and M-cones do for the + and –[L-M] directions, provided the relative S-cone excitation produced by the background is above ~9 units, see Figure 4 and Equation 6. Below this value, the relationship between the S-cone excitation produced by the background, and the change in S-cone excitation (δS) required for threshold, can be described by the power curve (Equation 7) (r^2 = 0.87). The background luminance levels that produced these low excitations ranged from 0.3 to 24 $cd.m^{-2}$ (i.e., some chromaticities displayed at low luminance levels can produce similar excitations in a particular cone class to different chromaticities displayed at high luminance levels). The two equations needed to predict the measured threshold excitation increments in S-cones as a function of background excitation are given below:

$$\delta S = 0.0501 S_b + 0.6452 \text{ for } S_b > 9 \qquad \text{(Equation 6)}$$
$$\delta S = 0.3168 S_b^{0.5627} \qquad \text{for } S_b \leq 9 \qquad \text{(Equation 7)}$$
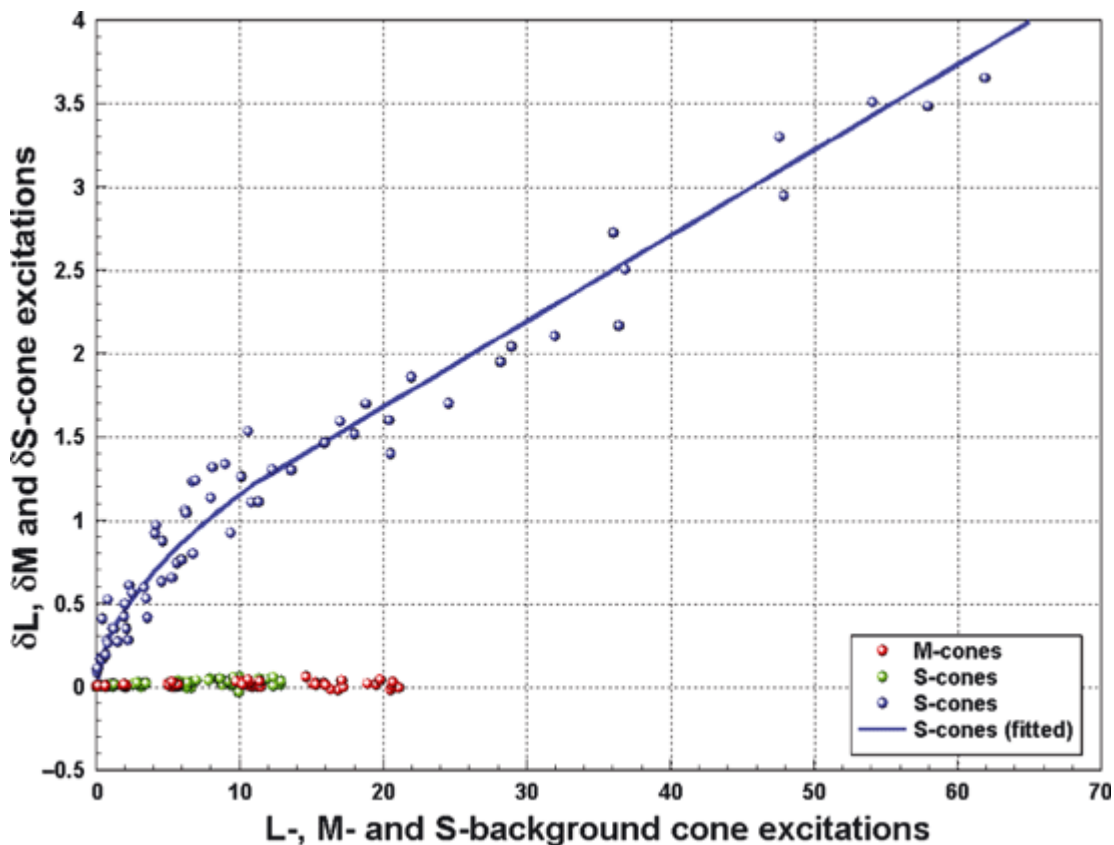

Figure 4
Change in S-cone excitation required to reach threshold in the +S direction vs the S-cone excitations produced by the backgrounds. The +S direction represents the mean orientation of the major axis of the threshold detection ellipse measured for each of the four subjects investigated in this study. The curve obeys a linear relationship (see Equation 6) for relative S-cone excitations above ~9 units and a power law relationship with a coefficient of 0.56 (see Equation 7) for cone excitations below this value. Note that the corresponding changes in L- and M-cones are approximately zero when thresholds are measured in the +S direction.

Figure 4 plots the measured S-cone increments at threshold as well as the predictions based on Equations 6 and 7. The corresponding changes in L- and M-cones in the blue direction have also been calculated and found to be negligible (see Figure 4). A similar method was used to produce equations that predict the S-cone excitation change required in the –S direction.

Reconstruction of ellipses

The orientation of the measured fitted ellipses in the [L-M]- vs S-cone excitation space, relative to the +[L-M] axis, is 90° ± 1.1° (mean ± S.D.). In view of this small variation, the assumption was made that all ellipses in the excitation space are aligned with their semi-major axes parallel to the S-cone excitation axis, consistent with Boynton et al. (1986) and Le Grand (1949). We calculated the change in cone excitation required for thresholds for each colour direction. Based on these thresholds and the 90° orientation, ellipse parameters were calculated.

When using Equations 2 and 3 to predict the total [L-M] excitation change in the +L-M direction, the mean error between measured data and predicted threshold excitations was 8.9% ± 6.2% (mean ± S.D.). The corresponding error in the –L+M direction was found to be 8.5% ± 7.1% (mean ± S.D.).

As the CIE 1931 diagram is popular and used in many industries (Shevell, 2003; Valberg, 2005) the ellipses were transformed back into CIE space using the inverse of Equation 1. The mean measured ellipse data (black dots) in CIE (x, y) space are shown for a range of background luminance levels: 1 (Figure 5); 3 (Figure 6); 8 (Figure 7) and 24 (Figure 8) cd.m^{-2}, respectively. The predictions of the model are shown as red contours.
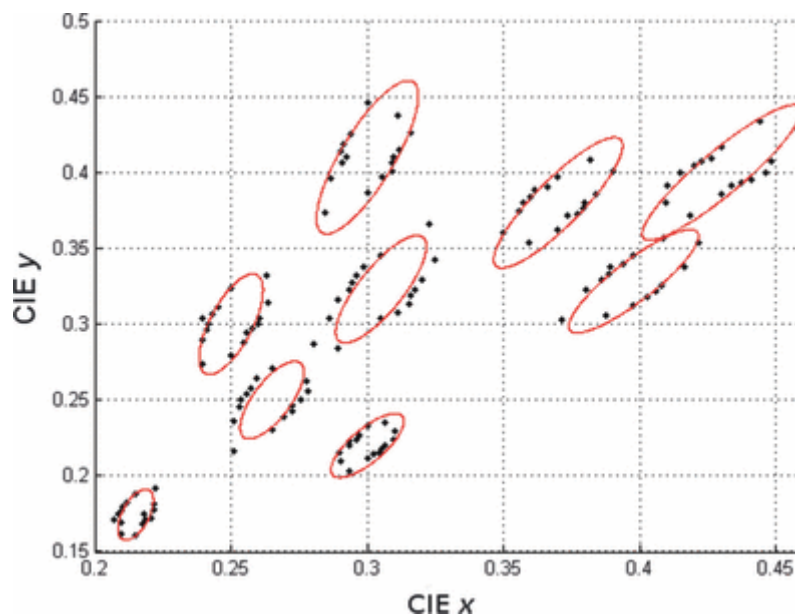

Figure 5

Model predictions of detection thresholds (shown in red) together with the measured thresholds (black dots) in the CIE 1931 space for a background luminance level of 1 cd m^{-2}.

Figure 6
Model predictions of detection thresholds (shown in red) together with the measured thresholds (black dots) in the CIE 1931 space for a background luminance level of 3 cd
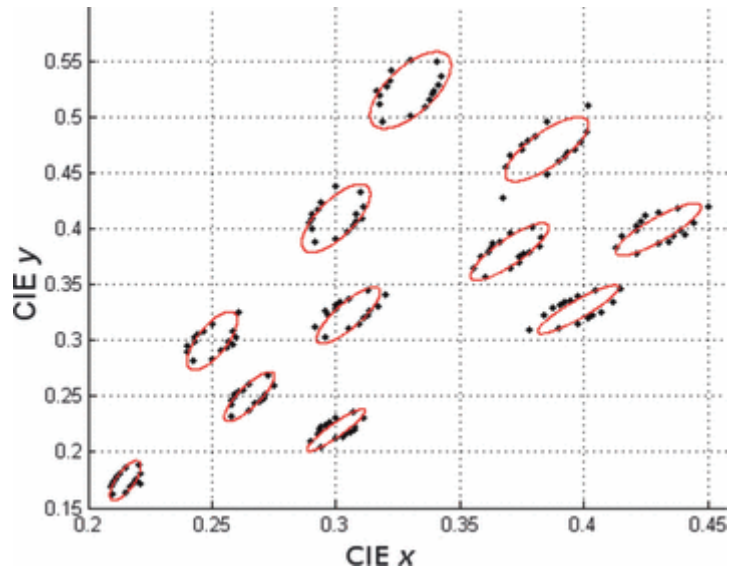m^{-2}.

Figure 7
Model predictions of detection thresholds (shown in red) together with the measured thresholds (black dots) in the CIE 1931 space for a background luminance level of 8 cd
m^{-2}.

Figure 8

Model predictions of detection thresholds (shown in red) together with the measured thresholds (black dots) in the CIE 1931 space for a background luminance level of 24 cd m^{-2}.
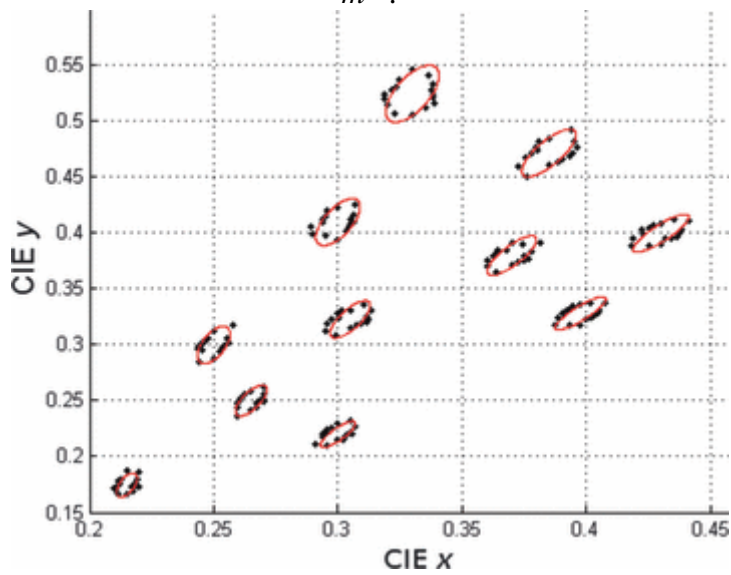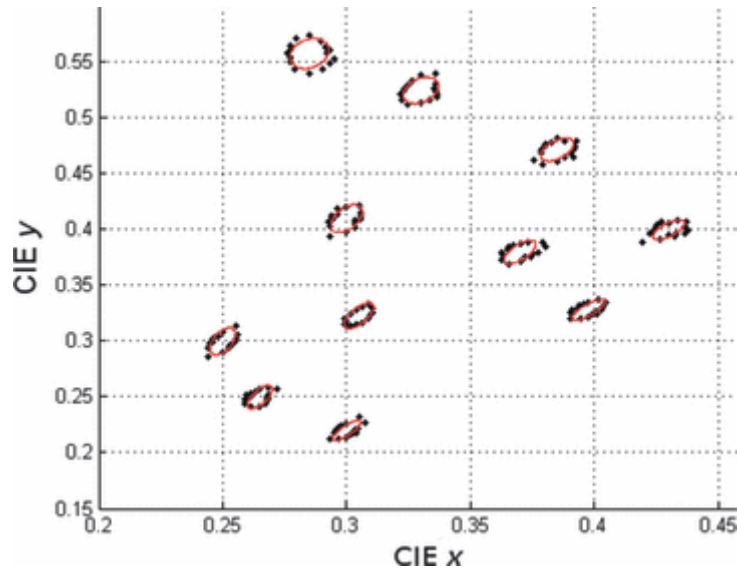
The predicted cone excitations required for threshold were compared to the corresponding excitations computed for the measured data to assess the differences between the measured and predicted thresholds. The results reveal the smallest differences for the +L-M direction and the largest differences for the +S direction (as outlined in Table 1).

Table 1. Mean and maximum (model predictions) cone excitation errors for each cone class in the +L-M and −S colour directions

Direction	Cone type	Mean	±	S.D. (%)	Maximum error (%)
+L-M	L	0.49	±	1.13	5.36
+L-M	M	1.27	±	2.80	13.13
+L-M	S	1.93	±	1.67	6.94
−S	L	0.67	±	1.32	6.46
−S	M	0.74	±	1.46	7.34
−S	S	4.51	±	2.55	9.57

The maximum errors occur when predicting the threshold excitations for the lowest background luminance level (0.3 cd.m^{-2}). These errors combine when ellipses are predicted in CIE space. Figure 9 shows the percentage differences between predicted and fitted ellipse parameters in CIE space as a function of background luminance. At luminance levels above 3 cd.m^{-2} there is no significant change in the accuracy of the predicted ellipse parameters. The mean errors for the predicted semi-major axes, semi-minor and orientation above 3 cd.m^{-2} are ~ 6.8%, 5.6% and 5.7%, respectively. Below 3 cd.m^{-2} the errors are larger, particularly for the semi-major axis of the ellipse, which also shows increased inter-subject variability in measured thresholds.
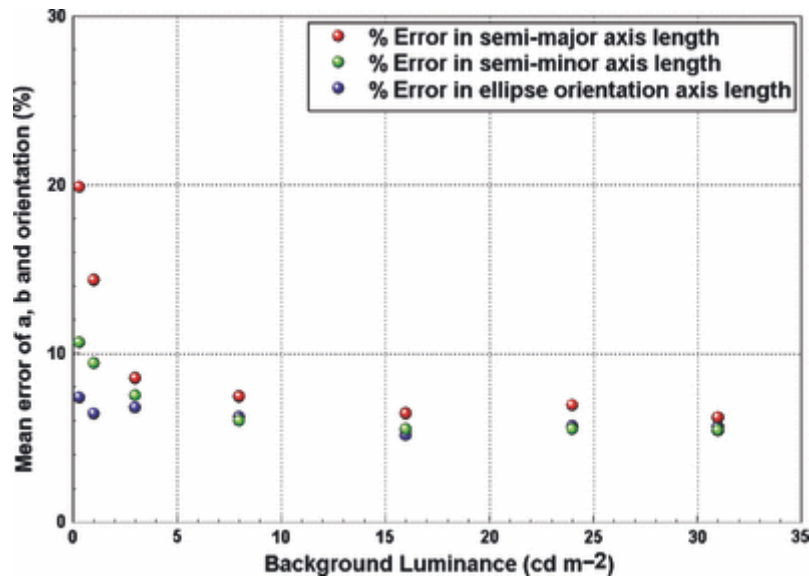
Figure 9

Mean errors for each set of predicted ellipse parameters (when grouped by background luminance level). Each error reflects the difference between the measured and the corresponding prediction for that parameter based on the mean fitted ellipse. The large errors are restricted to the semi-major axis and reflect the larger inter-subject variability in S-cone excitation at threshold.

Comparison with Macadam's ellipses

MacAdam (1942) performed an experiment in which observers made a series of colour matches. A fixed reference colour was presented and the observers' task was to adjust a second colour next to it in a 2° comparison field until it matched the reference colour. Using the same reference colour the observers made repeated colour matches along different directions in colour space and the standard deviations of the matches for a number of colour directions were calculated. It was discovered that plotting the standard deviations with respect to the reference colour on the CIE 1931 chromaticity diagram produced an ellipse. In total, 25 reference colours were used and hence 25 ellipses were produced. The reference and test fields were presented at a luminance of approximately 48 $cd.m^{-2}$: over the course of the experiment we have to assume that some chromatic adaptation to the stimulus occurred. Performing the same analysis on MacAdam's data we find similar relationships between the excitations produced by the reference field, and the change in cone excitations required to produce the standard deviations MacAdam measured in many directions. There is a significant difference in size between MacAdam's ellipses and the ellipses measured using the CAD test. This is largely due to the use of standard deviations estimated from repeated matches to quantify threshold changes in MacAdam's method, whereas the CAD test measures colour detection thresholds using a four-alternative, forced-choice procedure based on a two-down, one-up staircase method (Levine, 2000). If the MacAdam's ellipses are all scaled by ~4.5 along their semi-major and minor axis, the set of ellipses become comparable to those predicted by the model, although this is out of the luminance range of the model based on the luminance levels tests. Le Grand (1949) also analysed MacAdam's data for only one isoluminant plane investigated using two sets of cone fundamentals (König and Fick) to determine the corresponding cone excitations. Our results are largely consistent with Le

Grand's findings. Their analysis reveals similar changes in threshold S-cone excitation with S-cone background signal as demonstrated in our study. Le Grand also showed (using both sets of fundamentals) that the orientations of the ellipse's semi-major axes align themselves with the S-cone excitations axis (referred to as the 'B' axis).

Conclusion

We have shown that even when the differences in chromatic adaptation are large, a strong linear relationship exists between the background L-, M- and S-cone excitations, and the corresponding increments required for threshold in each colour direction. Based on the findings from this study, this relationship exists over at least ~2 log units for the L- and M-cones and slightly less for S-cones, but a correction can be applied at low light levels to extend the predictive range for S-cones. Using these derived relationships it is possible to predict the cone excitations required for threshold detection of colour signals along the +L-M, -L+M, +S and –S cardinal directions, at least within the chromaticity range and luminance levels associated with typical display applications. These excitations can be used to predict the discrimination ellipse parameters in CIE space with small errors of ~6% over most of the range. Predictions of yellow and blue thresholds are less accurate below 3 $cd.m^{-2}$, but these thresholds also show larger inter-subject variability when measured experimentally.

At a high background luminance level, the L-cone excitations of the stimulus in the red and green colour directions need only increase/decrease by ~0.4%; at the lower luminance levels the increase needed can be as large as ~1.4%. The M-cone stimulus excitation also only requires a small change for threshold in the +L-M and –L+M directions. A change of only ~0.65% is required at the highest light level; at the lowest light levels this change can be as large as ~2.3%. The S-cone excitation at threshold requires much larger changes (i.e., an increase/decrease of ~6%) relative to the signals generated in S-cones by the background for either the yellow or the blue colour directions. This change can be as large as ~25% for background luminance levels below 3 $cd.m^{-2}$.

The findings from this study suggest that the required changes in L- and M-cone excitations at threshold are small. The need for only small changes to reach threshold may account for the linear relationships observed in Figures 3 and 4, as well as the other cardinal directions. The same is true for the S-cones at background luminance levels above 3 $cd.m^{-2}$ for each condition of chromatic adaptation, even though S-cones require a slightly larger change in excitation to reach threshold. For the lower background luminance levels investigated (<3 $cd.m^{-2}$) the linear relationship derived for the S-cones (Equation 6) is no longer appropriate. S-cone excitations can still be predicted for the lower background excitation levels by applying Equation 7.

The data show that provided the background cone excitation in a particular cone class remains unaltered, changes in chromatic adaptation are equivalent to changes in luminance. The following example taken from the measured data helps to clarify this finding. The L-, M- and S-cone excitations produced by the background CIE (x, y): 0.305, 0.323 at a luminance of 24 $cd.m^{-2}$ are 15.976, 9.225, and 28.221, respectively. The L-, M- and S-cone excitations produced by the background CIE (x, y): 0.215, 0.175 at the lower luminance of 8 $cd.m^{-2}$ are 5.308, 3.515 and 28.976, respectively. Due to this particular difference in chromaticity and luminance there is a large difference in the L- and M-cone excitations that the two backgrounds produce (33.2% and 38.1% respectively). These two conditions of chromatic

adaptation produce almost identical S-cone excitations of 28.221 and 28.976 (a difference of only 2.6%). The S-cone excitation required for threshold in the +S direction for the first background is 30.169, and 31.015 for the second background (a difference of only 1.2%). There are also small differences in the S-cone excitation required for threshold in the +L-M, −L+M and −S directions between the two states of 1.0%, 1.2% and 0.1%, respectively.

These observations suggest that when threshold detection of coloured signals is involved, the state of chromatic adaptation only affects the measured thresholds through changes in absolute cone excitation levels. No significant interaction of signals generated in different cone classes is therefore involved. The results suggest that cone signal changes needed for threshold detection are always the same for a given background cone excitation level (in any cone class), independent of the excitation generated in the other cone classes.

References

Barbur, J. L. (2003) 'Double-blindsight' revealed through the processing of color and luminance contrast defined motion signals. Prog. Brain Res. 144, 243–259.

Barbur, J. L., Rodriguez-Carmona, M. and Harlow, J. A. (2006) Establishing the statistical limits of "normal" chromatic sensitivity: CIE Proceedings Expert Symposium – 75 Years of the CIE Standard Observer (CIE x030:2006), ISBN: 3901906517.

Boynton, R. M., Nagy, A. L. and Eskew, R. T. (1986) Similarity of normalized discrimination ellipses in the constant-luminance chromaticity plane. Perception 15, 755–763.

Brown, W. R. J. (1951) The influence of luminance level on visual sensitivity to Color Differences. J. Opt. Soc. Am. 41, 684–688.

Fitzgibbon, A., Pilu, M. and Fisher, B. (1999) Direct least squares fitting of ellipses. IEEE Trans. Pattern Anal. Mach. Intell. 21, 476–480.

Golz, J. and MacLeod, D. (2003) Colorimetry for CRT displays. J. Opt. Soc. Am. 20, 769–781.

Hita, E., Romero, J., Cervantes, A. and Delbarco, L. J. (1989) The influence of chromatic adaptation upon successive colour discrimination. J. Opt - Nouvelle Revue D'Optique 20, 87–94.

Hunt, R. W. (1998). Measuring Colour, 3rd edn. Fountain Press, Tolworth, ISBN 0863433871.

Le Grand, Y. (1949) Les Seuils Différentiels de couleurs dans la Théorie de Young. Rev. Opt. 28, 261–278.

Levine, M. W. (2000) Fundamentals of Sensation and Perception. Oxford University Press, Oxford, ISBN: 9780198524663.

Loomis, J. M. and Berger, T. (1979) Effects of chromatic adaptation on color discrimination and color appearance. Vision Res. 19, 891–901.

MacAdam, D. L. (1942) Visual sensitivities to color differences in daylight. J. Opt. Soc. Am. 32, 247–274.

Morovic, J. (2008). Color Gamut Mapping, 1st edn. John Wiley & Sons, Chichester, West Sussex, ISBN 9780470030325.

Rodriguez-Carmona, M. L., Harlow, J. A., Walker, G. and Barbur, J. L. (2005) The variability of normal trichromatic vision and the establishment of the "normal" range. Proceedings of 10th Congress of the International Colour Association. Granada 979–982.

Salomon, D. (2005). Curves and Surfaces for Computer Graphics. Springer, New York, ISBN-10: 0387241965.

Shevell, S. K. (2003). The Science of Color, 2nd edn. Elsevier, Oxford UK, ISBN 0444512519.

Stockman, A. and Sharpe, L. T. (2000) Spectral sensitivities of the middle- and long-wavelength sensitive cones derived from measurements in observers of known genotype. Vision Res. 40, 1711–1737.

Valberg, A. (2005). Light Vision Color. J Wiley & Sons, Chichester, West Sussex, ISBN 0470849037.

Walkey, H. C., Barbur, J. L., Harlow, A. J. and Makous, W. (2001) Measurements of chromatic sensitivity in the mesopic range. Colour Res. Appl. 26, 36–42.

Yebra, J. A., García, J. L., Nieves, J. and Romero, J. (2001) Chromatic discrimination in relation to luminance level. Colour Res. Appl. 26, 123–131.

Yeh, T., Pokorny, J. and Smith, V. C. (1993) Chromatic discrimination with variation in chromaticity and luminance: data and theory. Vision Res. 33, 1835–1845.